

Indanesulfonamides as Carbonic Anhydrase Inhibitors. Toward Structure-Based Design of Selective Inhibitors of the Tumor-Associated Isozyme CA IX

Anne Thiry,[†] Marie Ledecq,[†] Alessandro Cecchi,[‡] Jean-Michel Dogné,[†] Johan Wouters,[†] Claudiu T. Supuran,[‡] and Bernard Masereel^{†,*}

Drug Design and Discovery Center, University of Namur, 61 rue de Bruxelles, 5000 Namur, Belgium, and Polo Scientifico, Laboratorio di Chimica Bioinorganica, Rm. 188, Università degli Studi di Firenze, Via della Lastruccia 3, 50019 Sesto Fiorentino, Florence, Italy

Received January 10, 2006

Carbonic anhydrases are ubiquitous metalloenzymes which are involved in fundamental processes (i.e., acid–base regulation, respiration, calcification, etc.). The carbonic anhydrase isozyme IX becomes an interesting pharmacological target due to its overexpression in cancer and its absence in normal tissue. Therefore, several indanesulfonamides were synthesized and tested for their inhibition both against the human CA IX and against two other biologically relevant isozymes (CA I and II). Structure–activity relationships are discussed and point out different compounds for its selectivity and activity against CA IX. To establish preliminary hypothesis for the design of new isozyme-selective CA IX inhibitors, we conducted molecular modeling. We describe here the first human CA IX model built by homology with another CA isozyme already crystallized. Docking studies were performed to explore the binding mode of our indanesulfonamide derivatives.

Introduction

At least 13 enzymatically active α -carbonic anhydrase (CA, EC 4.2.1.1) isoforms have been discovered in higher vertebrates.^{1–4} These metalloenzymes are involved in the catalysis of an important physiological reaction: the hydration of CO₂ to bicarbonate and a proton (CO₂ + H₂O \leftrightarrow HCO₃[–] + H⁺). As a consequence, they regulate the pH, the secretion of electrolytes, and the respiration by their presence throughout neural pathways controlling ventilation.^{5–7} CAs also play a major role in biosynthetic pathways which require CO₂/bicarbonate as substrate such as gluconeogenesis, lipogenesis, ureagenesis, and pyrimidines synthesis.⁸ Other roles for these enzymes were highlighted, such as calcification and bone resorption.⁹ The discovery that CA IX, a transmembrane tumor-associated protein,¹⁰ was prevalently expressed in several human cancer cells and not in their normal counterparts¹¹ suggests a role for some CAs in oncogenesis.⁸ Several studies showed a clear-cut relationship between high CA IX expression levels in tumors and a poor prognosis.^{12,13} CA IX also acts on cells adhesion and differentiation by its N-terminal proteoglycan related-region which is absent in other transmembrane CA isozymes, such as CA XII and CA XIV.¹⁴

Tumor cells have a lower extracellular pH (pH_e) than normal cells.¹⁵ An acidic pH_e contributes to increase tumor progression by promoting the action of growth factors^{16,17} and proteases¹⁸ and an increased rate of mutation.¹⁹ Recently CO₂ and lactic acid were demonstrated as a significant source of acidity in tumors, pointing out the implication of CA in tumor progression.²⁰ The expression of CA IX is both regulated by the von Hippel-Lindau (VHL) tumor suppressor protein and by hypoxia present in some tumors. Thus, the inactivation of the VHL factor gene enhances the expression of CA IX,²¹ whereas hypoxia induces the expression of CA IX through a direct transcriptional

activation of CA9 gene by the hypoxia-inducible factor-1 (HIF-1).²² Moreover, hypoxia stimulates CA IX to decrease the pH_e (by an yet unknown mechanism of action) proving that the expression levels and the catalytic activity of CA IX are dependent on the availability of oxygen within the tumor.²³

CA IX is clearly implicated in the acidification of the pH_e as shown by Svastova et al.²³ Teicher and collaborators also demonstrated that acetazolamide (AZA) decreased the tumor growth *in vivo* and enhanced the action of some chemotherapeutic agents, such as cisplatin, melphalan, and PtCl₄, when used in combination therapy.²⁴ Several CA IX-selective sulfonamide inhibitors were able to reduce the extracellular acidification of Madin-Darby canine kidney (MDCK)-CA IX cells in hypoxia but not in normoxia.²³ Moreover, a decrease of the pH_e reduces the cytotoxicity of weakly basic chemotherapeutic drugs such as paclitaxel, mitoxantrone, and topotecan.²⁵ Taken together, these data increase the interest for selective CA IX inhibitors in cancer therapy. Such compounds may prevent the decrease of pH_e and may be used in combinations with other antitumor drugs to increase the efficacy or the uptake of weakly basic drugs.^{15,24} Thus, the aim of the present study is the design, synthesis, and *in vitro* pharmacological evaluation of original indanesulfonamides as selective CA IX inhibitors.

A series of indanesulfonamide derivatives was synthesized and tested for their inhibitory activity against CA IX, and against CA I and II, two other physiologically relevant CA isozymes. To better understand the structure–activity relationships (SAR) of this series, we present here the homology modeling of the isozyme IX based on CA XIV. This is the first CA IX model described and used to perform docking studies and to establish preliminary hypothesis for the design of new compounds.

Results and Discussion

Chemistry. To date, X-ray crystallographic structures are not available for CA IX thus preventing a structure-based design of selective CA IX inhibitors. The indanesulfonamide template was first described by our group as a potent inhibitor against

* Corresponding author. Phone, +32 81 72 43 38. Fax, +32 81 72 42 99. E-mail: bernard.masereel@fundp.ac.be.

[†] University of Namur.

[‡] Università degli Studi di Firenze.

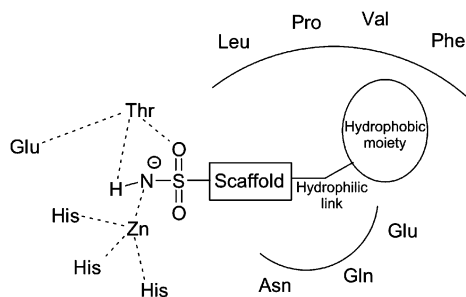
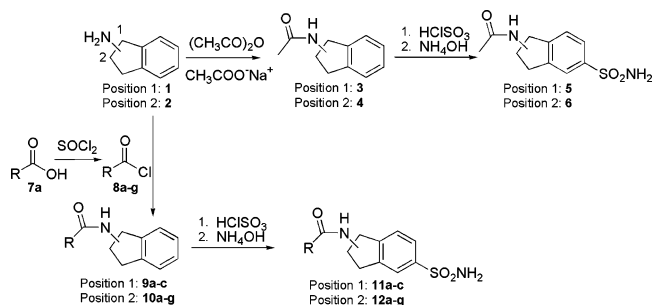


Figure 1. Structural elements of CA inhibitors in the CA enzymatic active site. A sulfonamide attached to the scaffold coordinates the zinc ion and interacts with threonine by H bond. The side chain might possess a hydrophilic link able to interact with the hydrophilic part of the active site and a hydrophobic moiety which can interact in the hydrophobic pocket.

Scheme 1. Synthesis of Indanesulfonamides from 1- or 2-Aminoindane



R = Valpropyl (a), cyclohexyl (b), pentafluorophenyl (c), ethyl (d), propyl (e), butyl (f), nonyl (g)

CA I and II.²⁶ On the basis of these preliminary results, we designed indanesulfonamide derivatives based on the recently described “tail approach”.^{3,27} A general pharmacophore was drawn (Figure 1) from the analysis of CAs active site and from the structure of inhibitors described in the literature.³ Figure 1 shows the structural elements required for the inhibition of CAs. A side chain which can interact with the hydrophobic and hydrophilic parts of the CA active site can substitute an aromatic or heterocyclic sulfonamide scaffold. Therefore, different hydrophobic side chains were incorporated in the indanesulfonamide scaffold with an amide linker which can interact with the hydrophilic part of the active site (Figure 1). The selected hydrophobic side chains (methyl, valproyl, cyclohexyl, and pentafluorophenyl) substitute the indane moiety in positions 1 or 2. Such hydrophobic chains incorporated in other scaffolds have already demonstrated a powerful CA inhibition.^{3,28,29} Racemic indanesulfonamides were synthesized following the Scheme 1. Moreover, investigation of the elongation of the side chain with a *n*-ethyl, *n*-propyl, *n*-butyl, and *n*-nonyl was performed in position 2 of the indane ring.

CA Inhibition. The inhibition activities of indanesulfonamide derivatives were evaluated against hCA I, II, and IX and are reported in Table 1. Acetazolamide was used as a standard inhibitor for comparison. As seen from Table 1, nearly all the derivatives show a high inhibitory potency against CA IX and CA II and a weak inhibition against CA I. The K_i ratios of CA I over CA IX reveal that compounds **5**, **12b**, **11c**, **12f**, and **12g** are selective against CA IX while the K_i ratios of CA II over CA IX point out that compounds **12b**, **11c**, **12f**, and **12g** preferentially inhibit CA IX. Among these selective CA IX inhibitors, **11c** is also characterized by a potent inhibitory potency against this isozyme.

The analysis of the K_i values obtained for CA IX can be summarized in two points. (i) The influence of the length of

Chart 1

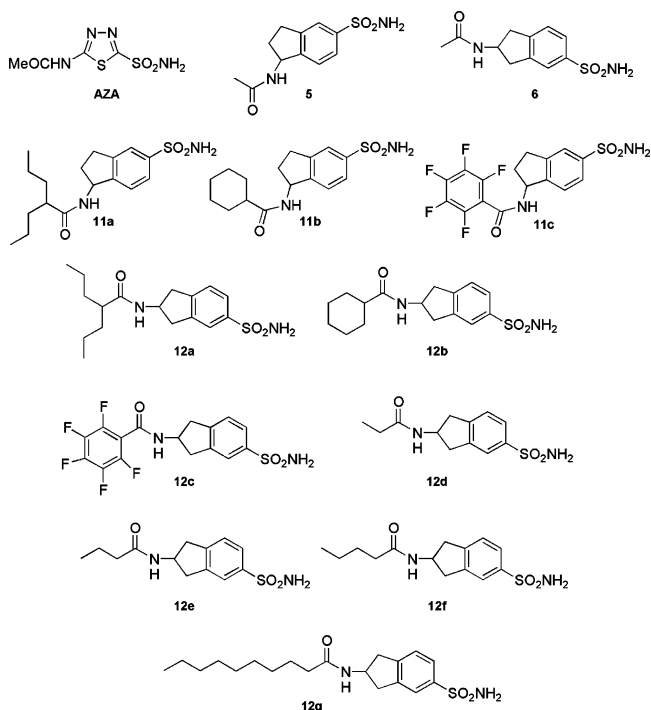


Table 1. Inhibition Data of Indanesulfonamide Derivatives and Standard Inhibitor Acetazolamide

compound	K_i (nM)			K_i ratios ^a	
	hCA I	hCA II	hCA IX	$K_i(\text{hCAI})/K_i(\text{hCAIX})$	$K_i(\text{hCAII})/K_i(\text{hCAIX})$
AZA	900	12	25	36	0.48
5	56500	186	193	292	0.964
6	2510	1.0	290	8.6	0.0034
11a	810	1.2	37.5	22	0.032
12a	4130	0.9	282	15	0.003
11b	880	32	108	8.1	0.30
12b	3560	118	30	118	3.9
11c	770	490	3.5	220	140
12c	600	6.7	33	18.2	0.20
12d	3440	10	2015	1.7	0.0050
12e	825	46	2320	0.35	0.020
12f	875	7.5	3.4	257	2.2
12g	5330	128	3.7	1440	35

^a The K_i ratios are indicative of the inhibition selectivity. A weak selective inhibitor is characterized by low K_i ratios.

the side chain on CA inhibition: a methyl provides a K_i of 290 nM (**6**). An additional carbon (**12d**, *n*-ethyl side chain) increases the K_i value (2015 nM), and the *n*-propyl side chain (**12e**) leads to a higher K_i value (2320 nM). Surprisingly, the inhibition becomes more efficient with a side chain containing four carbons (**12f**, *n*-butyl moiety) with a K_i of 3.4 nM. The *n*-nonyl moiety (**12g**) provides a comparable inhibition. We can conclude that the optimum length of the side chain for the design of new inhibitors seems to be about four carbons. (ii) Influence of the substitution pattern of the indanesulfonamide scaffold on CA inhibition revealed the following: a methyl group substituted in position 1 (**5**) or 2 (**6**) leads to the same range of inhibitory potency. With other substituents, some differences can be highlighted between the corresponding regioisomers (compare **11a–c** and **12a–c**). On one hand, position 1 seems to be favorable for a valproyl (**11a** vs **12a**) and a pentafluorophenyl group (**11c** vs **12c**). On the other hand, a cyclohexyl ring leads to a better inhibition constant when it is present in position 2 (**12b**).

Table 2. Selection of Template for CA IX. BLASTp Determination for the Identity Percentage of the Best Ranked Crystallized Proteins

protein	PDB code	identity percentage	E value
mCA XIV	1RJ5 ³²	38	2×10^{-52}
hCA XII	1JCZ ⁴⁵	36	2×10^{-49}
hCA II	1CA2 ⁴⁸	33	5×10^{-32}

We can conclude that sulfonamides **11c**, **12f**, and **12g** are potent CA IX inhibitors with a K_i value in the range of 3.4–3.7 nM. They are characterized by a good selectivity toward CA IX in comparison to CA I and CA II. In comparison with the reference drug AZA, these three drugs are more potent and selective for hCA IX than AZA.

Molecular Modeling

In an attempt to rationalize the high inhibitory activity and selectivity of compound **11c**, we conducted molecular modeling studies of the enzyme/inhibitor interaction. Similar studies were performed on the less active and less selective regioisomer **12c**. Due to the lack of experimental 3D data for CA IX, the first step was to build a model of this isozyme. The modeled active site was then used to investigate the interactions between CA IX and both regioisomers of **11c** and **12c**. We explored through docking studies, the binding mode of these two inhibitors.

1. Comparative Modeling. Three-dimensional (3D) protein structure is an important tool to highlight the function of a protein and the interaction with ligands. Homology (comparative modeling) is currently the most accurate method to predict the 3D structure of proteins when no experimental structure is available.³⁰ The modeling process generally consists of four steps: (1) databank search to identify the template, (2) target-template alignment, (3) model building and optimization, and (4) quality assessment of the resulting structure. To identify the template, the protein–protein BLAST algorithm³¹ was performed on the sequence of hCA IX. The identity percentage between hCA IX and several templates have been determined. Three CA isozymes with a 3D available structure provide the best ranking score (Table 2). Among them, murine CA XIV (mCA XIV, available on the Protein Data Bank of Brookaven, PDB, www.rcsb.org/pdb, PDB code 1RJ5)³² provides the best identity percentage (38%) and was chosen as template to build the CA IX model. The target-template alignment step is generally accepted as the most critical step in homology modeling.³³ Therefore, to improve the accuracy of this essential stage, a “consensus” alignment (Table 3) between the target and the chosen template was used with the aid of the automated

**Figure 2.** The final 3D model of hCA IX where α -helices are red and β -sheets are yellow. The active site is delimited by three histidines which coordinate the zinc ion.

program of homology modeling ESyPred3D.³⁰ All the key regions corresponding to the amino acids of the active site and the metal binding site were correctly aligned.

On the basis of this “consensus” alignment, a 3D model was built with the MODELLER program³⁴ (Figure 2). This final model was then evaluated against the Ramachandran plot³⁵ provided by the PROCHECK program.³⁶ Only two amino acids, Thr361 and Ser368 were found in the disallowed region of the Ramachandran plot. They are located in loops far from the active site and would probably not modify its topology. It is generally considered that if at least 90% of the amino acids are in the allowed region the quality of the model can be evaluated as good.³⁶ In this case, the model contains 98.4% of the amino acid in the allowed region and only 0.5% in the disallowed region. These results showed that our model is reliable for performing further docking studies.

2. CA IX Active Site Characterization. Superimposition of the 3D structure of hCA II available from the PDB (PDB code 1A42)³⁷ and hCA IX model is represented in Figure 3. Both active sites form a cone where the summit consists of the zinc ion coordinated to three histidine residues. Hydrophobic and hydrophilic pockets are also present. Amino acids of the active site¹ are highly conserved (Figure 3). Nevertheless, we can note three differences in the amino acid sequence of the active site of hCA IX as compared to hCA II: Thr205, Val262,

Table 3. Sequences Alignments Generated by ESyPred3D for Human CA IX (hCA IX) and the Template Murine CA XIV (mCA XIV)

		hhhh	ss	ss	sss	
hCAIX	141	WRYG---	GDPPWPRVSPACAGRFQSPVDIRPQLAAFCPALRPLELLGFQLPPLPE			192
mCAXIV	22	WYEGPHGQDHWPSTSYPECGGDAQSPINIQTDSVIFDPPDLPAVQPHGYDQLGTEP				76
		sssss	ssss	sss	ssssssssss	ss
hCAIX	193	LRLRNNGHSVQLTLPPLGLEMALGPGREYRALQLHLHWGAAGR-PGSEHTVEGHRF				246
mCAXIV	77	LDLHNNGHTVQLSLPPTLHLGGL-PRKYTAAQLHLHWGQRGSLEGEHHINSEAT				130
		ssssssss	hhhh	ssssssssss	hhhhhhh	
hCAIX	247	PAEIHVVHLST-AFARVDEALGRPGGLAVLAAPFLEEGPEENSAYEQLLSRLEEIA				300
mCAXIV	131	AAELHVVHYDSQSYSSLSEAAQKPQGLAVLGILIEVGETENPAYDHILSRLEHIR				185
		ssss	ssssss	ssssss	ssssss	ssshhh
hCAIX	301	EKGSETQVPGLDISALLPSDFSRYPQYEGSLTTPPCAQGVIVTFVFNQTVMLSAKQ				355
mCAXIV	186	YKDQKTSVPPFSVRELFPQQLQEQFFRYNGSLTTPPCYQSVLWTVFNRRQAISMGG				240
		hhhhh		ss		
hCAIX	355	LHTLSDTLWGPGRD---RLQLNFRATQPLNQRVIEASF*				390
mCAXIV	241	LEKLQETLSSTTEEDPSEPLVQNYRVPQPLNQRITIFASF*				278

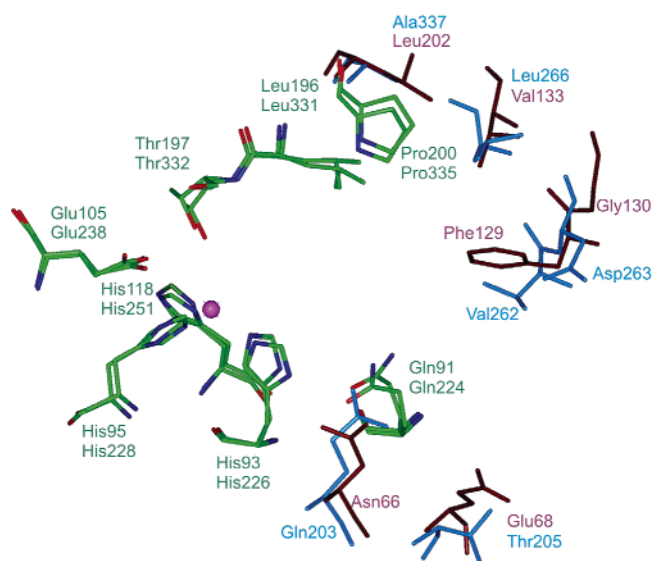


Figure 3. Superimposition of CA II and hCA IX active sites. The conserved active site residues are colored by atom; differences between amino acids of hCA IX and CA II are colored respectively in blue and in red.

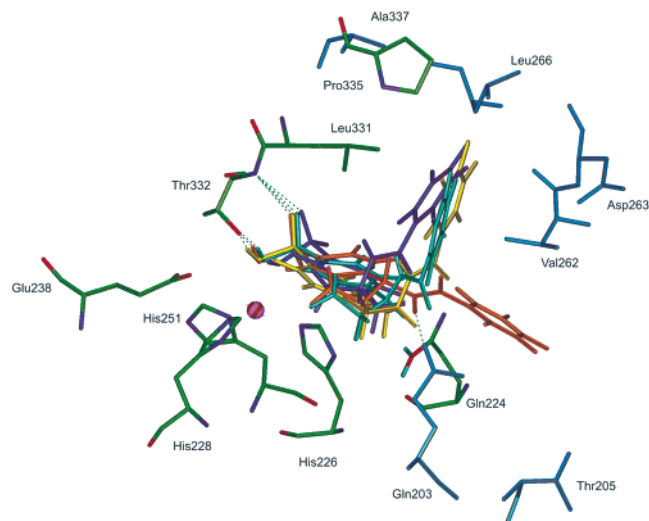


Figure 4. Interaction modes of **11c** and **12c** with hCA IX model after refinement of the best ranked docked solution. Specific hCA IX residues are colored in blue. Compound *S*-**11c** is represented in cyan, *R*-**11c** in orange, *S*-**12c** in dark blue, and *R*-**12c** in yellow. H bond are indicated in green dotted.

and Asp263 replace Glu68, Phe129, and Gly130 of hCAII, respectively. These differences are associated with a modification of some physicochemical properties. Moreover, those amino acids are known to be involved in the binding of inhibitors.³⁸ Therefore, these features are relevant for the design of selective CA IX inhibitors.

3. Docking. The docking program GOLD³⁹ (Genetic Optimization for Ligand Docking) was used to simulate the interaction between the inhibitors and the active site of CA IX model. Docking studies were carried out in order to understand why the incorporated pentafluorophenyl in position 1 on indane (**11c**) enhances by 10 fold the inhibitory constant in comparison with its regioisomer (**12c**). For each compound, *R* and *S* enantiomers were considered. All the compounds are anchored into the active site by the zinc complexation of the sulfonamide moiety (Figure 4). Indeed, sulfonamides are known to bind to the zinc ion in a tetrahedral adduct by substituting the nonprotein zinc ligand.¹ The docking studies modeled this major interaction

correctly. A hydrogen bond is established between the sulfonamide nitrogen atom and the hydroxyl moiety of Thr332. One of the oxygen atoms of the sulfonamide moiety is H-bonded with the backbone amide of Thr332. The hydrophobic side chain of the inhibitors interacts with the active site residues following two orientations. In the first, the pentafluorophenyl moiety of *S*-**11c**, *R*-**11c**, and *S*-**12c** forms a 90° dihedral angle with the indane moiety. It lies nearby residues Leu331, Ala337, Leu266. In the second, the pentafluorophenyl moiety of compound *R*-**11c** and the indane moiety are coplanar. In this case, the pentafluorophenyl moiety is surrounded by Asp263, Gln203, and Thr205. The carbonyl oxygen of *R*-**11c** makes an H bond with the backbone amide nitrogen of Gln203. This interaction could direct the hydrophobic substituent toward the three “specific” residues of the CA IX active site. Therefore, we can hypothesize that regarding the activity and selectivity of both racemics **11c** in comparison with their regioisomers **12c**, derivative *R*-**11c** could provide the best activity and selectivity against CA IX.

4. Design of New Selective CA IX Inhibitors. The development of selective CA IX inhibitors will be interesting either to avoid adverse effects due to the inhibition of other CAs and also to study the exact physiological role of this isozyme.²⁷ This goal is difficult to achieve due to the high similarity of the CA isozyme’s active site. Two approaches can be planned. Recently, the incorporation of a positively charged moiety which confers membrane-impermeability properties to the molecule has been developed.⁴⁰ Such compounds show improved selectivity for the targeted CA IX because they are confined in the extracellular compartment.²³ They can consequently inhibit only membrane-associated CA isozyme possessing an extracellular catalytic domain like CA IX but not the cytosolic CA isozymes (CA II).⁴¹ On the other hand, it is possible to target specifically the nonconserved residues of hCA IX active site. Three amino acids have been pointed out in our study: Val262, Asp263, and Thr205 (which correspond respectively to the Phe129, Gly130, and Glu68 residues of hCA II). In fact, several substitutions could be envisaged. (i) The presence of the Asp263 residue in hCA IX could be interesting for the design of new inhibitors. Indeed, the incorporation of a positively charged side chain could form an ionic interaction with this moiety and would enhance the selectivity. Moreover, it is interesting to note that such compound will not enter into the cell where CA I and CA II are located. (ii) Bulky groups should be chosen to avoid the interaction with the phenyl moiety of Phe129 present in CA II. (iii) Neutral groups which can form H bond with the hCA IX Thr205 could also enhance the selectivity. (iv) The amide group present in our molecules should be maintained to allow the formation of an additional H bond with hCA IX Glu203. Such interaction could compel the inhibitor to interact with specific residues of hCA IX.

Conclusion

The synthesis and the biological evaluation of racemic indanesulfonamide derivatives on hCA I, II, and IX are reported in this paper. Two indanesulfonamides derivatives, the 1-pentafluorophenylamidoindane-5-sulfonamide (**11c**) and the 2-nonylamidoindane-5-sulfonamide (**12g**), possess an interesting profile characterized by a high inhibitory potency and selectivity against hCA IX. In addition, we have performed homology modeling and docking studies to rationalize the observed activities and to design new selective inhibitors. Since the 3D structure of CA IX is not yet available, we have built a model for hCA IX by homology with a similar isozyme already crystallized. Alignment of sequences provides mCA XIV as the

best template for homology constructing. Our model was evaluated, and its quality can be considered as good. Docking studies were then performed in this model with the most active and selective inhibitors against CA IX, compound **11c**. The corresponding regioisomer (**12c**) which was less active and less selective was also docked to understand the SAR. Enantiomers *R* and *S* of **11c** and **12c** were considered. One binding mode was observed for both enantiomers of **12c**, but two different binding modes are reported for the enantiomers of **11c**. Compound *R*-**11c** established an additional H-bond with Gln203 and could place its the side chain toward the specific residue of the CA IX active site. Separating and determining the activity of each enantiomer will give supplementary information on these docking studies. Moreover comparison of the ubiquitous isozyme hCA II and the tumor associated CA IX active site have pointed out the hCA IX nonconserved active site residues Asp263 and Thr205. These residues could be specifically targeted for the design of new selective compounds.

We intend to test compound **11c** on MDCK cells in order to evaluate its ability to reduce the medium acidification.²³ Then we will also determine if **11c** can modify the cellular uptake of anticancer drugs and modulate the response of tumor cells to conventional chemo- and radiotherapy.^{15,42}

Experimental Section

General. Reagents and solvents are supplied by Acros Organics, Sigma-Aldrich, or Merck Eurolab. They are used without purification. Reactions are followed by TLC performed on a silica gel Merck 5544, and spots are revealed under 254 nm UV illumination. Melting points were performed on a Tottoli-Büchi Melting Point B540 in open capillary tubes and are uncorrected. ¹H NMR spectra were recorded on a JEOL JNM EX 400 at room temperature using DMSO-*d*₆ as solvent and tetramethylsilane as internal standard. Chemical shifts are expressed in δ (ppm) and coupling constants (*J*) in hertz. The abbreviations s = singulet, d = doublet, dd = doublet of doublet, t = triplet, m = massif, m = multiplet, q = quadruplet, br = broad were used throughout. Electron ionization mass spectra were recorded on an Agilent 1100 Series MSD trap SL. Elemental analyses (C, H, N, S) were performed on a ThermoFinnigan Flash EA 112 elemental analyzer.

Synthesis of Indanesulfonamides. General Procedure. Compounds **3** and **4** were prepared by reacting 3 g of 1- or 2-aminoindane (**1** or **2**) (22.5 mmol) with 1.85 g of sodium acetate (22.5 mmol) and 30 mL of acetic anhydride. The mixture was stirred at room temperature for 2 h and then concentrated under reduced pressure. The residue was extracted three times by chloroform (3 \times 50 mL). The organic layers were combined, washed with water, with HCl 1% (p/v), with Na₂CO₃ 5% (p/v), and with brine solution, and dried with MgSO₄.

Compounds **9a–c** and **10a–g**: 2 g of 1- or 2-aminoindane (**1** or **2**) (11.8 mmol) was dissolved in chloroform (15 mL). A small excess of the corresponding acid chloride (**8a–g**) (14.2 mmol) was added. If the acyl chloride is not commercially available, it was prepared from 2 g of the corresponding carboxylic acid (**7a**, 13.9 mmol) by refluxing with an excess of thionyl chloride (20 mL) for 1 h. The excess of SOCl₂ was evaporated under reduced pressure. At the end of the reaction between the acid chloride and the 1- or 2-aminoindane monitored by TLC, the residue was extracted three times by ether or chloroform (3 \times 50 mL). The organic layers were combined and washed several times with water, HCl 1% (p/v), Na₂CO₃ 5% (p/v), and brine solution. The organic extract was then dried upon MgSO₄ and evaporated under reduced pressure. The residue was purified by crystallization from ether/pentane or ethyl acetate/pentane.

Compounds **5**, **6**, **11a–c**, and **12a–g**: The substituted indane (1 equiv) was added to chlorosulfonic acid (18 equiv) at -60 °C under argon. The mixture remains under stirring for 2 h at room temperature. The mixture was carefully poured into a mixture of

ethyl acetate and ice to hydrolyze the excess of acid. The organic layer was isolated and rapidly evaporated under reduced pressure. The chlorosulfonyl compound was dissolved in THF and poured into an excess of an aqueous ammonia solution. The corresponding sulfonamide was crystallized from ethanol/water (1/1).

1-Acetamido-5-sulfonamidoindane (5). The title compound (585 mg, 3.34 mmol) reacted according to the general procedure previously described. Yield: 55.4%; Mp: 202.8–204.6 °C; Anal. (C₁₁H₁₄N₂O₃S) C, H, N, S.

2-Acetamido-5-sulfonamidoindane (6). The title compound (1.46 g, 8.36 mmol) reacted according to the general procedure previously described. Yield: 35%; Mp: 217.8–221.6 °C; Anal. (C₁₁H₁₄N₂O₃S) H, N; C: calcd, 51.95; found, 51.06; S: calcd, 12.61; found, 11.96.

1-Valproylamido-5-sulfonamidoindane (11a). The title compound (650 mg, 2.51 mmol) reacted according to the general procedure previously described. Yield: 30.6%; Mp: 205.9–207.2 °C; Anal. (C₁₇H₂₆N₂O₃S) C, H, N, S.

1-Cyclohexylamido-5-sulfonamidoindane (11b). The title compound (407 mg, 1.67 mmol) reacted according to the general procedure previously described. Yield: 46.5%; Mp: 198.9–202.1 °C; Anal. (C₁₆H₂₂N₂O₃S) C, H, N; C: calcd, 8.69; found, 8.14; S: calcd, 9.95; found, 9.14.

1-Pentafluorophenylamido-5-sulfonamidoindane (11c). The title compound (821 mg, 2.51 mmol) reacted according to the general procedure previously described. Yield: 56.5%; Mp: 241.5–243.9 °C; Anal. (C₁₆H₁₁F₅N₂O₃S) H, N, S; C: calcd, 47.29; found, 48.56.

2-Valproylamido-5-sulfonamidoindane (12a). The title compound (650 mg, 2.51 mmol) reacted according to the general procedure previously described. Yield: 40%; Mp: 101.2–105.6 °C.

2-Cyclohexylamido-5-sulfonamidoindane (12b). The title compound (611 mg, 2.51 mmol) reacted according to the general procedure previously described. Yield: 47%; Mp: 180–182.1 °C; Anal. (C₁₆H₂₂N₂O₃S) H, N; C: calcd, 59.60; found, 59.14; S: calcd, 9.95; found, 9.36.

2-Pentafluorophenylamido-5-sulfonamidoindane (12c). The title compound (1.09 g, 3.34 mmol) reacted according to the general procedure previously described. Yield: 16.6%; Mp: 174.7–177.1 °C; Anal. (C₁₆H₁₁F₅N₂O₃S) C, H, N, S.

2-Ethylamido-5-sulfonamidoindane (12d). The title compound (633 mg, 3.34 mmol) reacted according to the general procedure previously described. Yield: 51.3%; Mp: 179.1–181.0 °C; Anal. (C₁₂H₁₆N₂O₃S) C, H, N, S.

2-Propylamido-5-sulfonamidoindane (12e). The title compound (510 mg, 2.51 mmol) reacted according to the general procedure previously described. Yield: 23.2%; Mp: 188.5–190.7 °C; Anal. (C₁₃H₁₈N₂O₃S) H, N, S; C: calcd, 55.30; found, 54.56.

2-Butylamido-5-sulfonamidoindane (12f). The title compound (545 mg, 2.51 mmol) reacted according to the general procedure previously described. Yield: 21.8%; Mp: 131.5–133.2 °C; Anal. (C₁₄H₂₀N₂O₃S) H, N; C: calcd, 56.73; found, 56.15; S: calcd, 10.82; found, 10.03.

2-Nonylamido-5-sulfonamidoindane (12g). The title compound (921 mg, 2.51 mmol) reacted according to the general procedure previously described. Yield: 49%; Mp: 132.8–134.9 °C; Anal. (C₁₉H₃₀N₂O₃S) H, N, S; C: calcd, 62.26; found, 62.71.

CA Inhibition. CA I and II were supplied by Sigma-Aldrich. The recombinant CA IX enzyme was obtained as reported earlier by Vullo et al.⁴³ An SX.18MV-R Applied Photophysics stopped-flow instrument has been for assaying the CA CO₂ hydration activity assays.⁴⁴ Phenol red (at a concentration of 0.2 mM) was used as indicator, working at the absorbance maximum of 557 nm, with 10 mM HEPES (pH 7.5) as buffer, 0.1 M Na₂SO₄ (for maintaining constant the ionic strength), following the CA-catalyzed CO₂ hydration reaction for a period of 10–100 s. Saturated CO₂ solution in water at 20 °C was used as substrate. Stock solutions of inhibitor (1 mM) were prepared in distilled–deionized water with 10–20% (v/v) DMSO (which do not influence the measure at these concentrations), and dilutions up to 0.1 nM were done thereafter

with distilled–deionized water. To allow for the formation of the E–I complex, inhibitor and enzyme solutions were preincubated during 15 min at room temperature prior to assay. Enzyme concentrations were 1.0 μM for CA I and II and 0.1 μM for CA IX. Each experiment was done in triplicate. The values reported throughout the paper were calculated as described in the literature.⁴⁴

Molecular Modeling. Selection of Template. The human CA IX sequence was obtained from Swiss-Prot database (accession number Q16790). The identification of homologues of CA IX was performed by protein–protein BLAST algorithm (Basic Local Alignment Search Tool)³¹ through the Protein Data Bank (BLOSUM62 matrix). The program compares protein sequences to sequence databases and calculates the statistical significance of matches (*E* value). Murine CA XIV (PDB code 1RJ5, resolution of 2.81 Å)⁴⁵ was selected as the most appropriate template (sequence identity 38%).

Comparative Modeling. An automated homology modeling program, ESyPred3D,³⁰ was used to build the CA IX model. The sequence of the catalytic domain of CA IX (from amino acids 141 to 390) and the sequence of the CA XIV template were submitted to the program. This program allowed a new alignment methodology by comparing the results from various multiple alignment algorithms to derive a “consensus” alignment between the target sequence and the template. From the best alignment of template structure to target sequence, 3D model containing non hydrogen atoms were automatically obtained using the method implemented in MODELLER.³⁴ The resulting model was energy minimized using the ESFF force field (DISCOVER3/InsightII) after the addition of H atoms fixed at a physiological pH value of 7.4 and the coordination of the zinc ion in a tetrahedral geometry. The final model was then evaluated with PROCHECK³⁶ by performing a Ramachandran plot³⁵ (pseudo-resolution of 2.0 Å).

Docking. GOLD³⁹ is a genetic algorithm for docking flexible ligands into protein binding sites. The interaction sphere was centered in the active site and delimited by a 12 Å radius. A tetrahedral geometry was imposed on the zinc binding site. 30 solutions have been generated and ranked by GOLD score. An optimization of the conformation of the ligand–protein complex and the evaluation of the interaction energy has been performed by the DISCOVER3⁴⁶ module implemented in INSIGHTII⁴⁷ (ESFF force field, dielectric constant = 1^{*r}). The energetic minimization process is performed in two steps: the Steepest Descent algorithm, reaching a convergence of 10.0 kcal·mol⁻¹·Å⁻¹, followed by the Conjugate gradient to reach a final convergence of 0.01 kcal·mol⁻¹·Å⁻¹. First, all the atoms of the CA IX were held fixed, and only the orientation of the ligand was optimized. Then, the side chains of active site residues followed by their backbone were relaxed. A tethering restraint was applied on these atoms, to keep them from moving too far from their original positions. This restraint had a quadratic form with a constant force of 10 kcal·mol⁻¹·Å⁻¹ and was progressively decreased (scale factor of 0.5).

The corresponding docked compounds were built with BUILDER implemented in INSIGHTII.⁴⁷

Acknowledgment. A. Thiry is very indebted to the “Fonds pour la Formation à la Recherche dans l’Industrie et dans l’Agriculture (FRIA)” for the award of a research fellowship. This work was funded by a FNRS grant (Belgian National Fund for Scientific Research). This work was also partly supported by an EU grant of the sixth framework program (EUROXY project) to C.T.S.

Supporting Information Available: Ramachandran map of the CA IX model and ¹H NMR, MS spectroscopy, and microanalytical data for all synthesized compounds not included in the Experimental Section. This material is free of charge via the Internet at <http://pubs.acs.org>.

References

- Supuran, C. T. Carbonic Anhydrases: Catalytic and Inhibition Mechanisms, Distribution and Physiological Roles. *Carbonic Anhydrase. Its Inhibitors and Activators*; CRC Press: London, 2004; pp 1–23.
- Kivela, A. J.; Kivela, J.; Saarnio, J.; Parkkila, S. Carbonic anhydrases in normal gastrointestinal tract and gastrointestinal tumours. *World J. Gastroenterol.* **2005**, *11*, 155–163.
- Supuran, C. T.; Scozzafava, A.; Casini, A. Carbonic anhydrase inhibitors. *Med. Res. Rev.* **2003**, *23*, 146–189.
- Supuran, C. T.; Scozzafava, A. Carbonic anhydrase inhibitors and their therapeutic potential. *Exp. Opin. Ther. Pat.* **2000**, *10*, 575–600.
- Supuran, C. T.; Scozzafava, A.; Conway, J. *Carbonic Anhydrase. Its Inhibitors and Activators*; CRC Press: London, 2004.
- Chegwidden, W. R.; Carter, N. D.; Edwards, Y. H. *The Carbonic Anhydrases New Horizons*; Birkhäuser Verlag: Basel, Boston, Berlin, 2000.
- Swenson, E. R. Respiratory and renal roles of carbonic anhydrase in gas exchange and acid–base regulation. *The Carbonic Anhydrases New Horizons*; Birkhäuser Verlag: Basel, Boston, Berlin, 2000.
- Chegwidden, W. R.; Dodgson, S. J.; Spencer, I. M. The roles of carbonic anhydrase in metabolism, cell growth and cancer in animals. *The carbonic anhydrases New Horizons*; Birkhäuser Verlag: Basel, Boston, Berlin, 2000; pp 343–363.
- Hentunen, T. A.; Härkönen, P. L.; Väänänen, H. K. Carbonic anhydrases in calcified tissues. *The carbonic anhydrases New Horizons*; Birkhäuser Verlag: Basel, Boston, Berlin, 2000; pp 491–497.
- Pastorekova, S.; Zavadova, Z.; Kostal, M.; Babusikova, O.; Zavadova, J. A novel quasi-viral agent, MaTu, is a two-component system. *Virology* **1992**, *187*, 620–626.
- Zavadova, J.; Zavadova, Z.; Pastorekova, S.; Ciampor, F.; Pastorek, J.; Zelnik, V. Expression of MaTu-MN protein in human tumor cultures and in clinical specimens. *Int. J. Cancer* **1993**, *54*, 268–274.
- Giatromanolaki, A.; Koukourakis, M. I.; Sivridis, E.; Pastorek, J.; Wykoff, C. C.; Gatter, K. C.; Harris, A. L. Expression of hypoxia-inducible carbonic anhydrase-9 relates to angiogenic pathways and independently to poor outcome in non small cell lung cancer. *Cancer Res.* **2001**, *61*, 7992–7998.
- Chia, S. K.; Wykoff, C. C.; Watson, P. H.; Han, C.; Leek, R. D.; Pastorek, J.; Gatter, K. C.; Ratcliffe, P.; Harris, A. L. Prognostic significance of a novel hypoxia-regulated marker, carbonic anhydrase IX, in invasive breast carcinoma. *J. Clin. Oncol.* **2001**, *19*, 3660–3668.
- Zavadova, J.; Zavadova, Z.; Pastorek, J.; Biesova, Z.; Jezek, J.; Velek, J. Human tumour-associated cell adhesion protein MN/CA IX: identification of M75 epitope and of the region mediating cell adhesion. *Br. J. Cancer* **2000**, *82*, 1808–1813.
- Stubbs, M.; McSheehy, P. M.; Griffiths, J. R.; Bashford, C. L. Causes and consequences of tumour acidity and implications for treatment. *Mol. Med. Today* **2000**, *6*, 15–19.
- Xu, L.; Fidler, I. J. Acidic pH-induced elevation in interleukin 8 expression by human ovarian carcinoma cells. *Cancer Res.* **2000**, *60*, 4610–4616.
- Fukumura, D.; Xu, L.; Chen, Y.; Gohongi, T.; Seed, B.; Jain, R. K. Hypoxia and acidosis independently up-regulate vascular endothelial growth factor transcription in brain tumors in vivo. *Cancer Res.* **2001**, *61*, 6020–6024.
- Kato, Y.; Nakayama, Y.; Umeda, M.; Miyazaki, K. Induction of 103-kDa gelatinase/type IV collagenase by acidic culture conditions in mouse metastatic melanoma cell lines. *J. Biol. Chem.* **1992**, *267*, 11424–11430.
- Reynolds, T. Y.; Rockwell, S.; Glazer, P. M. Genetic instability induced by the tumor microenvironment. *Cancer Res.* **1996**, *56*, 5754–5757.
- Helmlinger, G.; Endo, M.; Ferrara, N.; Hlatky, L.; Jain, R. K. Formation of endothelial cell networks. *Nature* **2000**, *405*, 139–141.
- Ivanov, S. V.; Kuzmin, I.; Wei, M. H.; Pack, S.; Geil, L.; Johnson, B. E.; Stanbridge, E. J.; Lerman, M. I. Down-regulation of transmembrane carbonic anhydrases in renal cell carcinoma cell lines by wild-type von Hippel-Lindau transgenes. *Proc. Natl. Acad. Sci. U.S.A.* **1998**, *95*, 12596–12601.
- Wykoff, C. C.; Beasley, N. J.; Watson, P. H.; Turner, K. J.; Pastorek, J.; Sibtain, A.; Wilson, G. D.; Turley, H.; Talks, K. L.; Maxwell, P. H.; Pugh, C. W.; Ratcliffe, P. J.; Harris, A. L. Hypoxia-inducible expression of tumor-associated carbonic anhydrases. *Cancer Res.* **2000**, *60*, 7075–7083.

- (23) Svastova, E.; Hulikova, A.; Rafajova, M.; Zat'ovicova, M.; Gibadulinova, A.; Casini, A.; Cecchi, A.; Scozzafava, A.; Supuran, C. T.; Pastorek, J.; Pastorekova, S. Hypoxia activates the capacity of tumor-associated carbonic anhydrase IX to acidify extracellular pH. *FEBS Lett.* **2004**, *577*, 439–445.
- (24) Teicher, B. A.; Liu, S. D.; Liu, J. T.; Holden, S. A.; Herman, T. S. A carbonic anhydrase inhibitor as a potential modulator of cancer therapies. *Anticancer Res.* **1993**, *13*, 1549–1556.
- (25) Vukovic, V.; Tannock, I. F. Influence of low pH on cytotoxicity of paclitaxel, mitoxantrone and topotecan. *Br. J. Cancer* **1997**, *75*, 1167–1172.
- (26) Chazalotte, C.; Masereel, B.; Rolin, S.; Thiry, A.; Scozzafava, A.; Innocenti, A.; Supuran, C. T. Carbonic anhydrase inhibitors. Design of anticonvulsant sulfonamides incorporating indane moieties. *Bioorg. Med. Chem. Lett.* **2004**, *14*, 5781–5786.
- (27) Supuran, C. T.; Casini, A.; Scozzafava, A. Development of carbonic anhydrase inhibitors. *Carbonic Anhydrase. Its Inhibitors and Activators*; CRC Press: London, 2004; pp 67–147.
- (28) Scozzafava, A.; Menabuoni, L.; Mincione, F.; Briganti, F.; Mincione, G.; Supuran, C. T. Carbonic anhydrase inhibitors: perfluoroalkyl/aryl-substituted derivatives of aromatic/heterocyclic sulfonamides as topical intraocular pressure-lowering agents with prolonged duration of action. *J. Med. Chem.* **2000**, *43*, 4542–4551.
- (29) Masereel, B.; Rolin, S.; Abbate, F.; Scozzafava, A.; Supuran, C. T. Carbonic anhydrase inhibitors: Anticonvulsant sulfonamides incorporating valproyl and other lipophilic moieties. *J. Med. Chem.* **2002**, *45*, 312–320.
- (30) Lambert, C.; Leonard, N.; De Bolle, X.; Depiereux, E. ESyPred3D: Prediction of proteins 3D structures. *Bioinformatics* **2002**, *18*, 1250–1256.
- (31) Altschul, S. F.; Madden, T. L.; Schaffer, A. A.; Zhang, J.; Zhang, Z.; Miller, W.; Lipman, D. J. Gapped BLAST and PSI-BLAST: a new generation of protein database search programs. *Nucleic Acids Res.* **1997**, *25*, 3389–3402.
- (32) Whittington, D. A.; Grubb, J. H.; Waheed, A.; Shah, G. N.; Sly, W. S.; Christianson, D. W. Expression, assay, and structure of the extracellular domain of murine carbonic anhydrase XIV: implications for selective inhibition of membrane-associated isozymes. *J. Biol. Chem.* **2004**, *279*, 7223–7228.
- (33) Martin, A. C.; MacArthur, M. W.; Thornton, J. M. Assessment of comparative modeling in CASP2. *Proteins* **1997**, (Suppl 1), 14–28.
- (34) Sali, A.; Sanchez, R.; Badretinov, A. MODELLER: A program for Protein Structure Modeling Release 4, 1997.
- (35) Ramachandran, G. N.; Sasisekharan, V. Conformation of polypeptides and proteins. *Adv. Protein Chem.* **1968**, *23*, 283–438.
- (36) Laskowski, R. A. Procheck: a program to check the stereochemical quality of protein structures. *J. Appl. Crystallogr.* **1993**, *26*, 283–291.
- (37) Stams, T.; Chen, Y.; Boriack-Sjodin, P. A.; Hurt, J. D.; Liao, J.; May, J. A.; Dean, T.; Laipis, P.; Silverman, D. N.; Christianson, D. W. Structures of murine carbonic anhydrase IV and human carbonic anhydrase II complexed with brinzolamide: molecular basis of isozyme-drug discrimination. *Protein Sci.* **1998**, *7*, 556–563.
- (38) Menchise, V.; De Simone, G.; Alterio, V.; Di Fiore, A.; Pedone, C.; Scozzafava, A.; Supuran, C. T. Carbonic anhydrase inhibitors: stacking with Phe131 determines active site binding region of inhibitors as exemplified by the X-ray crystal structure of a membrane-impermeant antitumor sulfonamide complexed with isozyme II. *J. Med. Chem.* **2005**, *48*, 5721–5727.
- (39) Jones, G.; Willett, P.; Glen, R. C.; Leach, A. R.; Taylor, R. *Gold*; 1.2 ed.; Astex Technology: Cambridge, UK.
- (40) Casey, J. R.; Morgan, P. E.; Vullo, D.; Scozzafava, A.; Mastrolorenzo, A.; Supuran, C. T. Carbonic anhydrase inhibitors. Design of selective, membrane-impermeant inhibitors targeting the human tumor-associated isozyme IX. *J. Med. Chem.* **2004**, *47*, 2337–2347.
- (41) Scozzafava, A.; Briganti, F.; Ilies, M. A.; Supuran, C. T. Carbonic anhydrase inhibitors: synthesis of membrane-impermeant low molecular weight sulfonamides possessing in vivo selectivity for the membrane-bound versus cytosolic isozymes. *J. Med. Chem.* **2000**, *43*, 292–300.
- (42) Pastoreková, S.; Pastorek, J. Cancer-related carbonic anhydrase isozymes and their inhibition. *Carbonic anhydrase. Its Inhibitors and Activators*; CRC Press: London, 2004; pp 255–281.
- (43) Vullo, D.; Franchi, M.; Gallori, E.; Antel, J.; Scozzafava, A.; Supuran, C. T. Carbonic anhydrase inhibitors. Inhibition of mitochondrial isozyme V with aromatic and heterocyclic sulfonamides. *J. Med. Chem.* **2004**, *47*, 1272–1279.
- (44) Khalifah, R. G. The carbon dioxide hydration activity of carbonic anhydrase. I. Stop-flow kinetic studies on the native human isoenzymes B and C. *J. Biol. Chem.* **1971**, *246*, 2561–2573.
- (45) Whittington, D. A.; Waheed, A.; Ulmasov, B.; Shah, G. N.; Grubb, J. H.; Sly, W. S.; Christianson, D. W. Crystal structure of the dimeric extracellular domain of human carbonic anhydrase XII, a bitopic membrane protein overexpressed in certain cancer tumor cells. *Proc. Natl. Acad. Sci. U.S.A.* **2001**, *98*, 9545–9550.
- (46) Accelrys, *Discover3*; Version 2.98 ed.; Accelrys Inc.: San Diego, 1998.
- (47) Accelrys, *InsightII*; Accelrys Inc.: San Diego, 2000.
- (48) Eriksson, A. E.; Jones, T. A.; Liljas, A. Refined structure of human carbonic anhydrase II at 2.0 Å resolution. *Proteins* **1988**, *4*, 274–282.